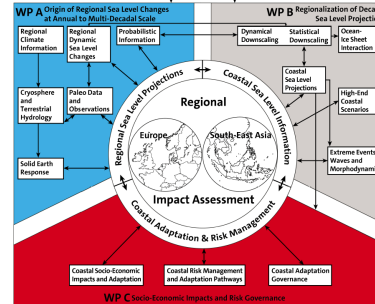




Highlights Ocean 2019-2020

AG Oceanography, Uni Bremen



Heat and Freshwater Transport by Mesoscale Eddies in the Southern Subpolar North Atlantic

Vasco Müller, Dagmar Kieke, Paul G. Myers, Clark Pennelly, Reiner Steinfeldt, and Ilaria Stendardo

The Mesoscale eddies in the ocean have a typical size of 100 km and a typical lifetime in the order of several days to several months. They cover around 25–30% of the ocean surface at any given moment. Since individual eddies can carry water trapped inside their cores and transport the properties of these waters over long distances, eddies are believed to significantly contribute to the horizontal transport of mass, heat, and salt throughout the ocean.

Sea level anomaly observations obtained from satellite altimetry provide the means of identifying and tracking eddies using automated algorithms. Combining these with sea surface temperature and salinity observations from satellites allows to analyse their surface signatures and to quantify horizontal surface fluxes. However, investigating the vertical structure of eddies and quantifying the respective heat and freshwater transports associated with the eddies are more challenging due to the lack of adequate subsurface observations on mesoscale resolutions.

Temperature (T) and salinity (S) fields for the deeper ocean are typically obtained from ship surveys and profiling Argo floats that are both limited in space and time. In a recent study (Müller et al., 2019) done in collaboration with scientists from the University of Alberta, Edmonton, Canada, we used a new gridded 3-dimensional data set of horizontal and vertical distributions of oceanic T/S fields. These fields were reconstructed from satellite altimetry data for the period

January 1993 to April 2014. This data set, available at daily resolution on a $1/4^\circ$ grid, was combined with sea level anomaly observations from the ocean surface that allowed to identify and track mesoscale eddies in the subpolar North Atlantic between 40°N – 55°N and 43°W – 20.5°W (Figure 71).

The North Atlantic between 40° – 55°N is influenced by two vastly different regimes of currents and water masses: the subpolar gyre, a large-scale cyclonic circulation cell, and the anticyclonic circulation cell of the subtropical gyre. In the Newfoundland Basin, the Western Boundary Current and the North Atlantic Current (NAC), the northward continuation of the Gulf Stream, flow in different directions along the boundary of the two gyres. The Western Boundary Current that originates in the north transports cold and fresh water of subpolar origin towards the tropics. The NAC, on the other hand, carries warmer and saline surface and subsurface waters of subtropical origin into the North Atlantic. It is this exchange of subpolar and subtropical waters that we are interested in.

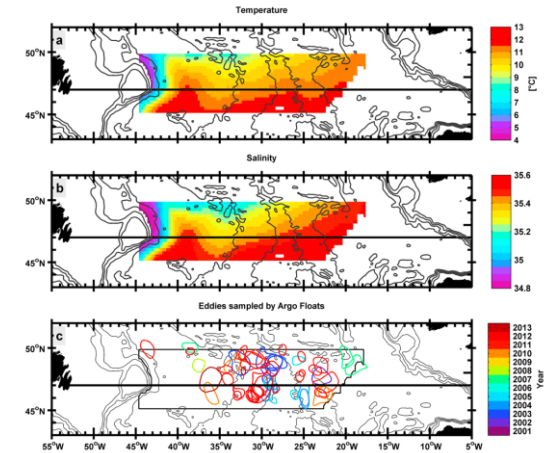


Figure 71: Average upper ocean (surface to 700 m) temperature (a) and salinity (b) in the region of interest shown for the period January 1993 to April 2014. The black line indicates the section at 47°N . Panel (c) shows all eddies that were sampled by individual Argo floats between 2001 and 2013. The limited data coverage as revealed by the Argo floats in (c) demonstrates the need for high-resolution hydrographic data sets as shown in (a) and (b).

We thus identified mesoscale eddies in our region of interest and assigned a vertical temperature and salinity profile to each of the eddies. This way, we were able to quantify the heat and freshwater transports for these eddies as they crossed the latitude of 47°N in northern or southern direction, which marks the approximate boundary between the subtropical and the subpolar regime.

We found that the largest heat and freshwater transports by eddies could be observed in the western part of the Newfoundland Basin. Around 35–45% of the heat and freshwater transports by eddies across 47°N stemmed from individual isolated eddies with large thermohaline signatures. Northward moving cold and fresh cyclonic eddies carrying subpolar water from the Western Boundary Current made a considerable contribution to the overall heat and freshwater transport by eddies crossing 47°N. While the transport by individual eddies was negligible compared to the transport by the mean flow in this region, we found a notable influence on the temporal variability.

We repeated the analysis based on data output obtained from a Canadian ocean model simulation that was based on the Nucleus for European Modelling of the Ocean (NEMO) modelling framework: the Arctic Northern Hemisphere Atlantic configuration with 1/4° horizontal resolution (ANHA4) with a nested 1/12° horizontal resolution encompassing the subpolar North Atlantic, called ANHA4-SPG12. The model simulation covered the period 2002-2013. The results obtained from the observational data sets were well reproduced in the model simulation; in particular, the modelled number of eddies crossing 47°N, the spatial distribution, and the associated heat and freshwater transports across this latitude were consistent with the observations.

Overall, the results from our study helped to provide a better understanding of the contribution of eddies to the transports of heat and freshwater and their variability in a region that is of great relevance for the climate system. The consistency between the observational data set and the model simulation shows that our results are physically meaningful. While there are still limitations regarding the availability of high-quality observations that are well resolved in space and time, model simulations that reasonably well reflect mesoscale dynamics can be used to study thermohaline transports by eddies in regions that may be less well covered by observations.

This study was carried out in the framework of the German-Canadian international research training group ArcTrain, funded by the German Research Foundation (DFG).

References

Müller, V., D. Kieke, P. G. Myers, C. Pennelly, R. Steinfeldt, and I. Stendero, I., Heat and freshwater transport by mesoscale eddies in the southern subpolar North Atlantic, *J. Geophys. Res.*: Oceans, 124, 5565–5585, doi:10.1029/2018JC014697, 2019.

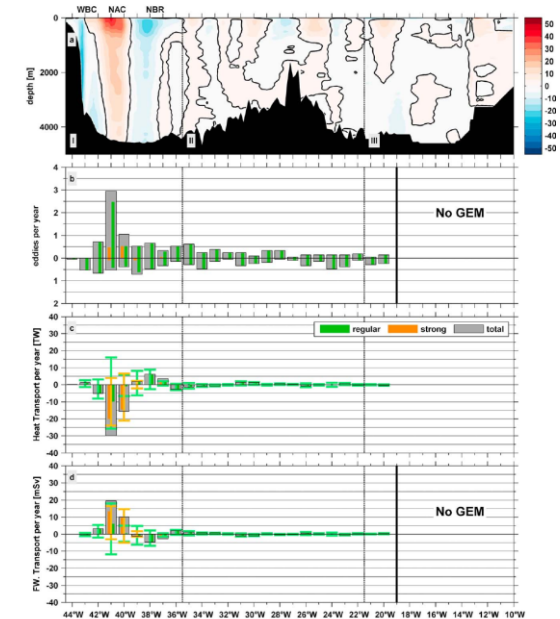


Figure 72: (a) Meridional background velocity obtained from 11 ship surveys conducted nominally along 47°N (from Müller et al., 2017), (b) the number of northward and southward moving eddies from satellite observations (January 1993 to April 2014) per 1° bin crossing 47°N per year, and (c) the sum of the heat and freshwater transports (d) by eddies per 1° bin along 47°N (normalized by the number of years). Vertical bars show the sum of the transports of regular (green) and strong (orange) eddies in either direction. The vertical whiskers represent the standard deviation of the respective transports in either direction. “No GEM” means, the required high-resolution 3D information of temperature and salinity is not available in this region.

Interannual and decadal variability of volume and freshwater transport of the NAC in the subpolar gyre

I. Stendardo, M. Rhein, and R. Steinfeldt

The North Atlantic Current (NAC) supplies the subpolar gyre with warm and saline water from the subtropics as part of the upper branch of the Atlantic Meridional Overturning Circulation (AMOC). Along its northward pathway, the NAC separates into several branches that move eastwards crossing the mid-Atlantic ridge (MAR) and supply the eastern Atlantic with subtropical water from the western basins.

We reconstructed salinity and velocity fields using a transfer function between sea surface height measured by remote sensing and salinity and temperature profiles from Argo floats. The result is a continuous record of salinity and velocity in the upper 1900m on a $1/4^\circ$ Cartesian grid with daily resolution starting in 1993. In general, long-term trends in the data are hidden by the strong interannual variability. As a surprise, the southernmost circulation branches originating near the Mann Eddy occasionally contribute volume and freshwater to the subpolar gyre, and most likely play an important role in the eastern Atlantic salinity distribution (Figure 73). Up to now, these branches were thought to recirculate back to the subtropical gyre and be of no consequence for the subpolar gyre. It turned out that the variability of the NAC-related freshwater transports in the western subpolar North Atlantic is as high, or even higher than the freshwater fluxes from the Arctic Ocean and thus needs to be considered when discussing the impact of freshwater fluxes on the subpolar North Atlantic.

Furthermore, we found that the salinity maximum is usually not found in the NAC but further east in the southward-flowing recirculation. We interpreted this feature being caused by lateral mixing of polar freshwater from the southward flowing western boundary current into the NAC (Figure 75). In this way 0.2 to 0.6 Sv freshwater from the western boundary are reintroduced into the subpolar gyre with the NAC (Figure 74).

Reference

Stendardo, I., Rhein, M., & Steinfeldt, R., The North Atlantic and its volume and freshwater transports in the subpolar North Atlantic, time period 1993-2016. *Journal of Geophysical Research: Oceans*. 125, e2020JC016065, doi:10.1029/2020JC016065, 2020.

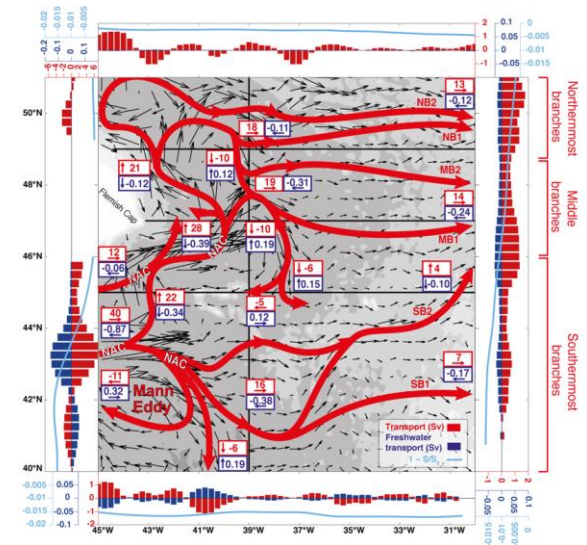


Figure 73: Map of reconstructed mean geostrophic velocities in the upper 700 m averaged over 1993–2015 (black arrows). Red: North Atlantic Current (NAC) branches and recirculation pathways based on these data. Red numbers: mean net northward/eastward (positive) or southward/westward (negative) volume transport for each NAC branch. Blue numbers: corresponding freshwater transports with directions (blue arrows) calculated using a reference salinity $S_0 = 34.80$. At the edges of the map, the zonal/meridional net volume (red bars) and freshwater (blue bars) transports are represented for each latitude/longitude grid point with a bar plot and the term $(1 - S/S_0)$ with a light blue line.

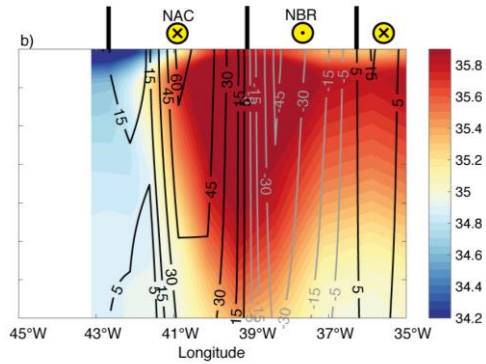


Figure 75: Salinity (contour colour) and velocity (contour lines) at 47°N in 2009 from our reconstructed dataset. Black: northward, grey: southward velocities. The southward flow is named Newfoundland Basin recirculation (NBR). Note that parts of the northward-flowing North Atlantic Current (NAC) are less saline than the recirculation.

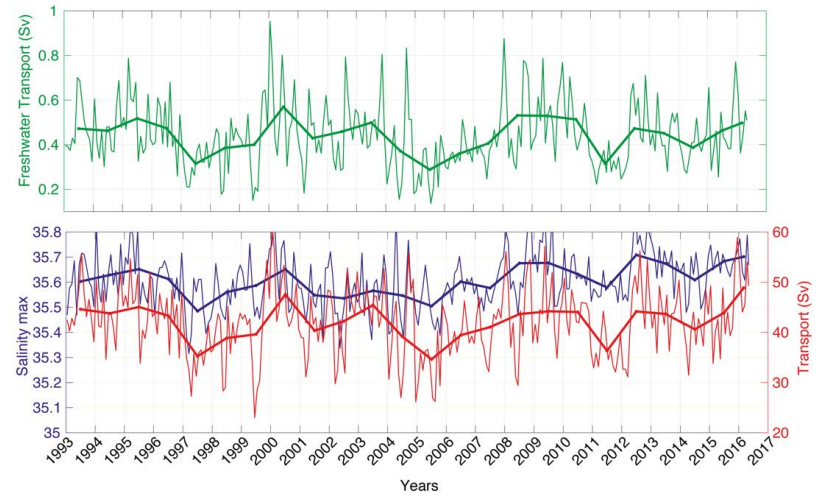


Figure 74: Time series of the NAC freshwater transport (Sv) (green lines, upper panel) at 47°N between 45°W and 37°W. Blue: maximum salinity between 45°W and 37°W in the upper 700 m used as reference salinity to calculate the freshwater transport (green). Red: NAC volume transport (Sv). Thick lines: annual means, thin lines: monthly means.

Wind-driven internal gravity waves

Georg S. Voelker, Dirk Olbers, Christian Mertens, and Maren Walter

Atmospheric cyclones with strong winds significantly impact ocean circulation, regional sea surface temperature, and deep water formation across the global oceans. Thus, they are expected to play a key role in a variety of energy transport mechanisms. Even though wind-generated internal gravity waves are thought to contribute significantly to the energy balance of the deep ocean, their excitation mechanisms are only partly understood. Most of the energy supply by wind is expected to be dissipated in the ocean surface layer and used there for mixing and entrainment.

In an idealized experiment, Voelker et al. (2019) studied the generation of internal gravity waves during a geostrophic adjustment process using an axisymmetric Boussinesq model forced by an idealized pulse of cyclonic wind stress. In this model, internal gravity waves are generated after approximately one inertial period. The outward radial energy flux is dominated by waves having structure close to vertical mode-1 and with frequency close to the inertial frequency. Less energetic higher mode waves are observed to be generated close to the sea floor underneath the storm. The total radiated energy corresponds to approximately 0.02% of the wind input. A deeper mixed-layer or weaker stratification further reduce this fraction. The low energy transfer rates suggest that other processes that drive vertical motion like surface heat fluxes, turbulent motion, mixed region collapse and storm translation are essential for significant energy extraction by internal gravity waves to occur.

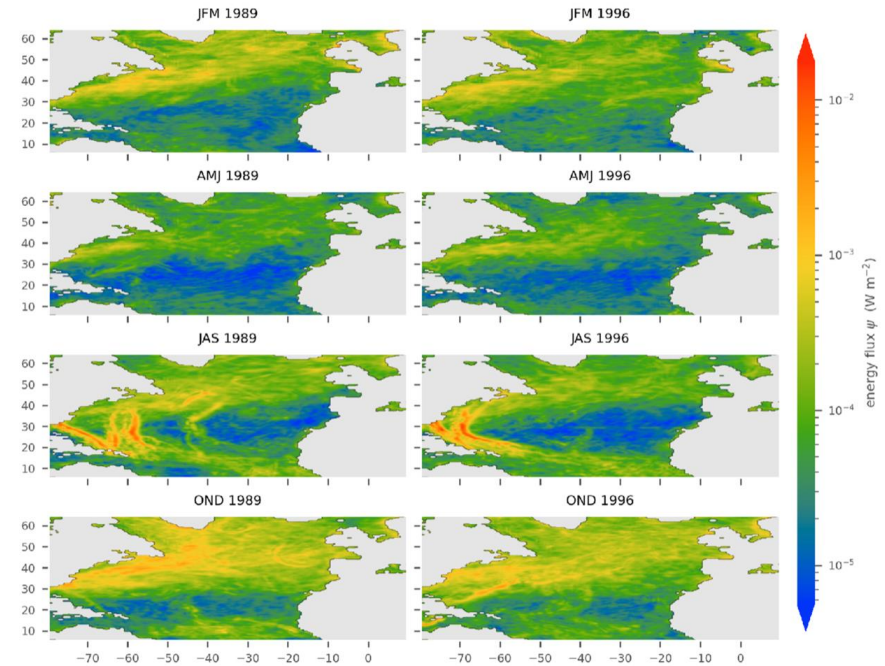


Figure 76: Seasonally averaged energy flux from the mixed layer into the internal wave field for a year with positive (1989, left) and negative (1996, right) NAO index computed with the hybrid extension. Figure from Voelker et al., 2020.

The fraction of the radiated flux to the surface flux of energy is of particular interest to ocean modellers. The radiative energy flux at the mixed layer base determines how much energy can be converted to turbulence in the interior of the ocean and made available for mixing the stratification. An analytical slab model of the mixed layer used before in several studies was extended by consistent physics of wave radiation into the interior. The extended model predicts the energy transfer rates, both in physical and wavenumber-frequency space, associated with the wind forcing, dissipa-

tion in the mixed layer, and wave radiation at the base as function of a few parameters. The results of the model are satisfactorily validated with a realistic numerical model of the North Atlantic Ocean (Olbers et al., 2020). An application of the slab model extension to the North Atlantic using NCEP-CFSR reanalysis wind data (Voelker et al., 2020) shows that the energy transfer into the interior is characterized by a high spatial and temporal variability determined by the wind structure, and dominated by extreme events like storm tracks (Figure 76). The average ratio of radiated energy fluxes from the mixed layer to near-inertial wind power is approximately 12%.

Hydrothermal plume studies using noble gas isotopes

Maren Walter, Florian Schmid, Janna Köhler, Christian Mertens, Maïke Peters, Andreas Türke, and Jürgen Sültenfuß

Helium is one of the gases carried from the Earth's mantle into the ocean by hydrothermal fluids. The absolute concentration of helium is hence much enhanced in the vicinity of hydrothermal vents. Primordial helium is enriched in ^3He compared to atmospheric sources, and the isotopic signature, the $^3\text{He}/^4\text{He}$ ratio, of primordial helium is significantly different from the atmospheric ratio. The concentration and isotopic composition of helium can be identified with high precision in water samples. As an inert noble gas, its concentration in the sea water is only altered by physical processes as mixing, not by biochemical interaction or scavenging. The isotopic signature of the primordial helium is detectable over long distances, which makes helium an ideal tracer to study the dispersal of hydrothermal material.

The oceanic crust is initially cooled and deep-sea chemosynthetic ecosystems are largely fed by hydrothermal circula-

Projects

IRTG ArcTrain (DFG) , TRR 181 Energy Transfer (DFG)

References

Olbers D, Jurgenowski P, Eden C, A wind-driven model of the ocean surface layer with wave radiation. *Ocean Dynamics*, 70, 1067–1088, 2020.

Voelker GS, Olbers D, Walter M, Mertens C, Myers PG, Estimates of wind power and radiative near-inertial internal wave flux —The hybrid slab model and its application to the North Atlantic—. *Ocean Dynamics*, 70, 1357–1376, 2020.

Voelker GS, Myers PG, Walter M, Sutherland BR, Generation of oceanic internal gravity waves by a cyclonic surface stress disturbance. *Dyn. Atmos. Oceans*, 86, 116-133, 2019.

tion and venting on the seafloor. Much of this venting takes place at mid-ocean ridges and in order to both make realistic models of the crust's thermal budget and to understand chemosynthetic biogeography, it is important to have a detailed inventory of vent sites. A major gap in this inventory was the Mid-Atlantic Ridge south of 13°S, a key region for vent fauna biogeography linking the Atlantic to the Indian and Pacific Oceans. During Maria S Merian cruise MSM25 we systematically surveyed the axial region between 13°S and 33°S for hydrothermal signals in the water column (Schmidt et al., 2019). The survey covered more than 2000 km of ridge crest, and we identified previously unknown hydrothermal plumes that indicate 14 new hydrothermal vent fields (Figure 77a). A wide gap in the distribution of vents in

the 19°S-23°S region coincides with the Rio de Janeiro Transform, the maximum southward progression of North Atlantic Deep Waters, and the maximum northwards extent of ^3He -enriched waters with Pacific origins (Figure 77b). Cross-flowing currents in the transform and the large gap between adjacent vents may prevent a meridional connection between the vent fauna communities in the North Atlantic and along the Antarctic Ridges, making this region a prime target for future biogeographical studies.

Compared to mid-ocean-ridge hydrothermal vent fields, those at intra-oceanic island arcs are typically in shallower water depth and have a more variable geochemical fluid composition. Shallow vent sites could influence the photic zone more directly and thus are potentially more relevant for marine primary productivity. The Kermadec arc in the SW Pacific is a very volcanically active part of the Pacific 'Ring of Fire', with more than 80 submarine and subaerial volcanoes. The RV Sonne cruise SO253 was carried out to study the chemically diverse hydrothermal systems hosted by volcanoes with different summit depths and their contribution to the local ecosystem. Helium isotopes in combination with a suite of other tracers as well as current measurements were used to infer the dispersal of the hydrothermal discharge at Brothers volcano, and contributed to one of the first estimates of chemical fluxes from arc systems (Neuholz et al., 2020a,b).

Projects

Hydrothermadec (BMBF), RidgeMix (DFG)

References

Neuholz R, Schnetger B, Kleint C, Koschinsky A, Lettmann K, Sander S, Türke A, Walter M, Zitoun R, Brumsack H-J, Near-field hydrothermal plume dynamics at Brothers Volcano (Kermadec Arc): A short-lived radium isotope study. *Chem. Geol.*, 533, 119379, 2020a.

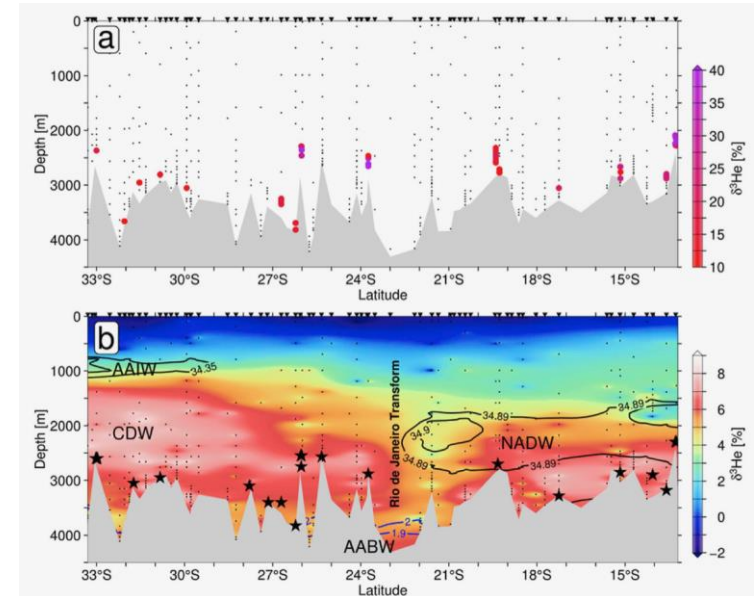


Figure 77: Two aspects of the ^3He distribution above the SMAR. (a) Hydrothermally sourced anomalies with $\delta^3\text{He} > 10\%$. Samples with $\delta^3\text{He} < 10\%$ are shown in black. (b) Gridded meridional section $\delta^3\text{He}$ background (samples with $\delta^3\text{He} > 9\%$ omitted from gridding). Contour lines delineate salinities/temperatures indicative of water mass cores: North Atlantic Deep Water (NADW), Antarctic Bottom Waters (AABW), and Antarctic Intermediate Water (AAIW); CDW denotes Circumpolar Deep Waters carrying excess $\delta^3\text{He}$ from the Pacific. Black stars indicate locations of identified hydrothermal vent sites. Figure from Schmid et al., 2019.

Neuholz R, Kleint C, Schnetger B, Koschinsky A, Laan P, Middag R, Sander S, Thal J, Türke A, Walter M, Zitoun R, Brumsack H-J, Submarine hydrothermal discharge and fluxes of dissolved Fe and Mn, and He isotopes at Brothers Volcano based on radium isotopes. *Minerals*, 10, 969, 2020b.

Schmid F, Peters M, Walter M, Devey C, Petersen S, Yeo I, Köhler J, Jamieson JW, Walker S, Sültenfuß J, Physico-chemical properties of newly discovered hydrothermal plumes above the Southern Mid-Atlantic Ridge (13°-33°S). *Deep Sea Res. I*, 148, 34-52, 2019.

Sensitivity of Labrador Sea Water Formation to Changes in Model Resolution, Atmospheric Forcing, and Freshwater Input

Yarisbel Garcia-Quintana, Peggy Courtois, Xianmin Hu, Clark Pennelly, Dagmar Kieke, and Paul G. Myers

The subpolar North Atlantic is a vital area for heat and freshwater exchange between the low and high latitudes. Within the subpolar North Atlantic, the Labrador Sea, located between the Labrador coast of Canada and Greenland, exerts a significant influence on the climate system. Strong winter cooling of the ocean surface causes the surface waters to lose heat to the atmosphere and to enable a process called deep convection. The Labrador Sea is one of the few regions in the world ocean where winter-time deep convection is known to occur. As a consequence the surface water becomes denser, the mixed layer starts to deepen, and the water sinks to depths between 500 and 2500 m. This sinking brings dissolved gases like oxygen and carbon dioxide into the deep ocean. The resulting water mass is known as Labrador Sea Water (LSW). Once formed, LSW spreads out from its formation region loaded with high concentrations of dissolved oxygen and anthropogenic tracers and can be tracked throughout the entire North Atlantic and beyond.

The process through which LSW is formed is sensitive to freshwater inflow into the formation region and storms passing over the Labrador Sea. While an increase in freshwater would inhibit the densification and sinking of surface water, fewer storms would reduce heat loss also reducing

the ability of the surface waters to gain in density and sink to greater depths. These are all changes projected to occur due to the ongoing anthropogenic climate change.

By using a numerical model, we investigated in our recent study (Garcia-Quintana et al., 2019) how changes in the spatial model resolution, the increase in freshwater discharge from Greenland, changes in the precipitation, and the absence of storms could impact LSW formation. This study was done in collaboration with scientists from the University of Alberta, Edmonton, Canada.

In order to explore the sensitivity of the LSW formation rate on changing conditions, a control simulation and four perturbation experiments were carried out using a Canadian state-of-the-art coupled ocean-sea ice model. The model simulation was based on the Nucleus for European Modelling of the Ocean (NEMO)

modelling framework, in particular the Arctic Northern Hemisphere Atlantic configuration with $1/4^\circ$ horizontal resolution (ANHA4). Each of the perturbation experiments had a specific alteration compared to the control simulation (Figure 78). LSW formation rates were determined using a

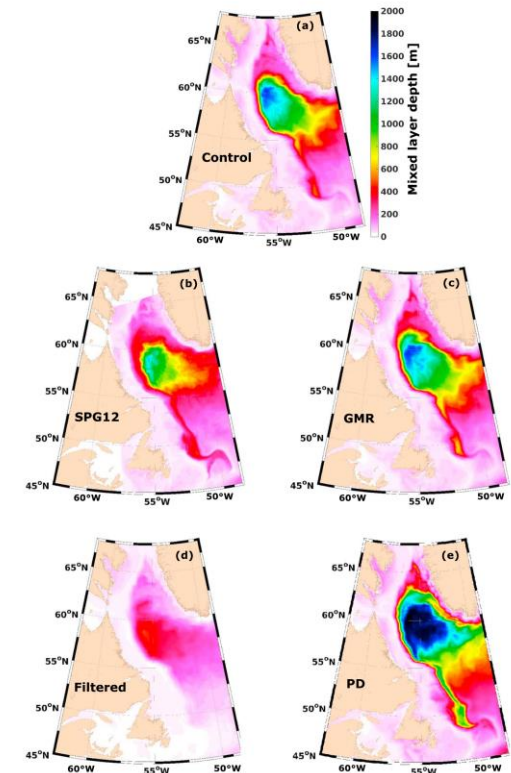


Figure 78: March mixed layer depths in the Labrador Sea, averaged over the years 2004 to 2016, for the control model simulation (a) and four perturbation runs (b-e). SPG12: increased spatial resolution of the model, GMR: Greenland meltwater discharge removed, Filtered: storms removed, PD: precipitation decreased.

kinematic subduction approach. The study considered the period from January 2004 to December 2016.

We found that by having more freshwater going into the formation region the overall LSW formation rate did not decrease, however, the water mass became lighter. Thus, the presence of Greenland meltwater affected mainly the formation of a denser type of LSW. In the absence of the storms, i.e., when removing all storms in the perturbation run, a decrease of 44% in heat loss over the Labrador Sea was noted, strong enough to halt the deep convection and decrease the LSW formation rate by 89%. Even if this exper-

Decay of internal tides

Janna Köhler, Jonas Löb, Maren Walter, Christian Mertens, Dirk Olbers, and Monika Rhein

Low-mode internal waves in the ocean possess a simple vertical structure, and hold a large part of the total energy of the internal wave field. They are able to travel basin-wide before they are dissipated (for a review, see Mertens et al. 2019). The spatial distribution of mixing related to internal wave dissipation affects the global overturning circulation in numerical models, but the observation as well as the representation of internal waves in ocean general circulation models (OGCMs) is still challenging. OGCMs do not resolve the spatial scales of the energy dissipation of internal waves and the resulting mixing. In order to account for mixing in the interior of the ocean, parameterizations have to be used. The module IDEMIX (Internal wave Dissipation Energy and Mixing) is a parameterization that describes the generation, propagation, interaction, and dissipation of the internal gravity wave field developed for the use in OGCMs (Olbers et al., 2019). IDEMIX is central to the concept of energetically consistent ocean models, since it links all sources and sinks of internal wave energy, as well as param-

eterized forms of energy, in a model without spurious sources and sinks.

We studied the radiated low mode internal waves including processes operating along their paths to improve our understanding of the life cycle of internal waves. To identify sources and sinks, as well as to quantify the contribution to local dissipation, in-situ hydrographic measurements were combined with observations of internal wave energy fluxes based on satellite altimetry and STORMTIDE. STORMTIDE is a 1/10°-simulation from the Max-Planck Institute Ocean Model (MPIOM) forced by the full lunisolar tidal potential that resolves low-mode internal waves. A realistic surface forcing with 6-hourly wind stress was included in STORMTIDE2, currently the only global OGCM that is driven by tidal and wind forcing. The region of in-situ observations was south of the Azores in the NE Atlantic, where the satellite altimetry and STORMTIDE show beams of converging low mode internal waves generated at a seamount chain.

Reference

Garcia-Quintana, Y., P. Courtois, X. Hu, C. Pennelly, D. Kieke, and P. G. Myers, Sensitivity of Labrador Sea Water formation to changes in model resolution, atmospheric forcing, and freshwater input, *J. Geophys. Res.: Oceans*, 124. doi:10.1029/2018JC014459, 2019.

The modal structure of the internal tide energy flux is important for the ratio of local (close to the generation site) to remote energy dissipation, as low-mode internal waves are less prone to breaking and more likely to propagate over large distances compared to waves with a complex vertical structure. Our in-situ observations show that even close to the generation site, the energy flux is primarily contained in the first mode and thus likely to propagate over long distances before dissipating (Köhler et al. 2019). Superposition of modes 1 and 2 captures over 84% of the total energy flux, indicating that OGCMs that resolve the first two modes are potentially able to capture the main characteristics of internal tide energy fluxes related to topography on scales typical for seamounts.

The direct comparison of the energy fluxes from the in-situ measurements, satellite altimetry, and OGCM shows that in-situ fluxes are generally higher than the corresponding fluxes in STORMTIDE and those derived from altimetry (Figure 79). Differences between in-situ data and altimetry are expected since the spatial resolution of satellite data limits the resolution of the inferred energy fluxes. The long-range propagation of the internal tides observed in altimetry generally agrees with the results from the in-situ measurements, although the in-situ energy fluxes are more variable and show a less monotonic decrease away from the generation sites. STORMTIDE resolves small scale structures in the energy flux distribution, but high energy fluxes are restricted to the vicinity of the generation sites.

While the study region was chosen because of the unimpaird spreading of internal tides after generation, a mooring time series reveals the presence of eddies during two time periods (Figure 80, Löb et al. 2020): one surface intensified eddy with a maximum horizontal velocity of approx. 20 cm s⁻¹, and a weaker subsurface one. The temporal variability

in the time series of energy flux is dominated by two factors: A strong coupling of the flux magnitude to the spring-neap variability in the barotropic tidal forcing (Figure 80), and the decrease of energy flux during phases of higher eddy kinetic energy. Especially the surface-intensified eddy is correlated with a significant weakening of the energy flux compared to the time period with no eddy activity (Figure 80). A potential transfer of the “missing” internal tide energy in modes 1 and 2 into higher mode internal waves would result in a changed ratio of local to remote energy dissipation and hence be important for the global distribution of internal wave energy.

A theoretical study on the energy transfer from the M2 internal tide to the ambient wave field via nonlinear triad interactions (Olbers et al. 2020) infers a globally integrated energy transfer of less than 0.1 TW for the STORMTIDE simulation, and up to 0.3 TW for a more energetic scenario. This compares reasonably well to 0.5 to 1 TW of global barotropic to baroclinic tidal conversion, but also suggests that other mechanisms such as local dissipation and tide-eddy interaction are important contributors to the global internal M2-tide energy sink. Whether the decrease in the low-mode

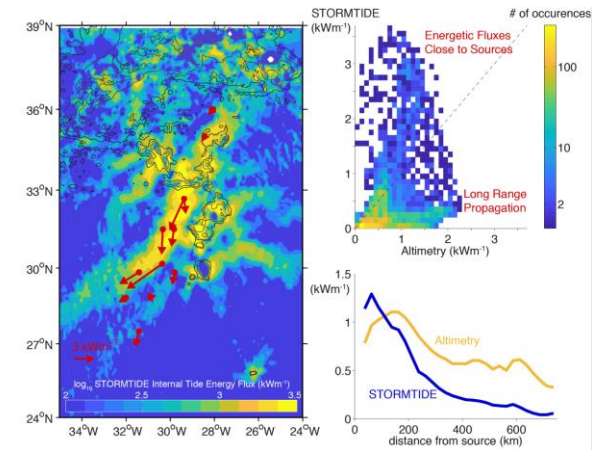


Figure 79: (left) M2 internal tide energy flux from in-situ observations (red arrows) and STORMTIDE (background); (right) comparison of internal tide energy fluxes in STORMTIDE and from satellite altimetry: STORMTIDE shows high values close to the generation sites, while in the altimetry higher fluxes persist over longer distances.

internal tide energy flux observed in the mooring time series is due to increased dissipation, refraction or scattering of energy into higher modes is the subject of a planned future study.

This research was conducted in the framework of the Collaborative Research Centre TRR 181 “Energy Transfer in Atmosphere and Ocean” funded by the Deutsche Forschungsgemeinschaft (DFG, German Research Foundation)—Projektnummer 274762653

References

Löb, J., Köhler, J., Mertens, C., Walter, M., Li, Z., von Storch, J.-S., Zhao, Z., Rhein, M., Observations of the low-mode internal tide and its interaction with mesoscale flow south of the Azores. *J. Geophys. Res. Oceans*, 125(11), e2019JC015879, 2020.

Olbers, D., F. Pollmann, C. Eden, On PSI Interactions in Internal Gravity Wave Fields and the Decay of Baroclinic Tides. *J. Phys. Oceanogr.*, 50, 751–771, 2020.

Köhler, J., Walter, M., Mertens, C., Stiehler, J., Li, Z., Zhao, Z., von Storch, J.-S., and Rhein, M., Energy Flux Observations in an Internal Tide Beam in the Eastern North Atlantic. *J. Geophys. Res. Oceans*, 124(8), 5747-5764, 2019.

Olbers, D., Eden, C., Becker, E., Pollmann, F., Jungclaus, J., The IDEMIX Model: Parameterization of Internal Gravity Waves for Circulation Models of Ocean and Atmosphere. In *Energy Transfers in Atmosphere and Ocean (87- 125)*, Carsten Eden and Armin Iske, Eds., Springer, 2019.

Mertens, C., Köhler, J., Walter, M., von Storch, J.-S., Rhein, M., Observation and models of low mode internal waves in the ocean. In *Energy Transfers in Atmosphere and Ocean (127- 143)*, Carsten Eden and Armin Iske, Eds., Springer, 2019.

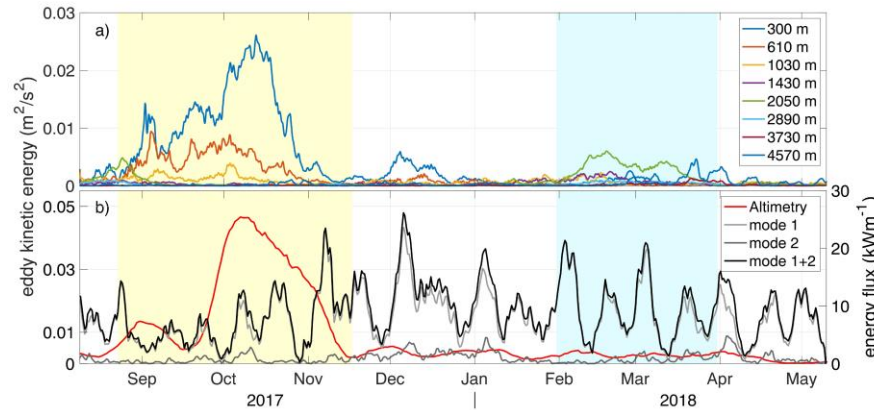


Figure 80: (a) Eddy kinetic energy (EKE) at the mooring location (30.48°N, 30.12°W) from the moored current meters and from CMEMS satellite data (red line in b). (b) Modal decomposition of observed energy flux of the semidiurnal internal tide. Different background colours indicate eddy activity: yellow = surface eddy; blue = subsurface eddy; white = no eddy. From Löb et al. 2020.

Observed transport decline at 47°N in the western North Atlantic

Monika Rhein, Christian Mertens, and Achim Roessler

The flow of warm and saline subtropical water toward the northern North Atlantic, a major component that makes northwestern Europe the warmest place in at these latitudes in winter, is part of the Atlantic meridional overturning circulation (AMOC). Climate models project an AMOC decline between 10% and 50% till 2100 with severe impacts on climate and sea level. Whether the AMOC has already weakened in response to anthropogenic climate change is an open question that motivates multiple sustained observation systems of the AMOC (Rhein 2019; McCarthy et al., 2020; Frajka-Williams et al., 2019).

Despite the importance of the large-scale circulation in the North Atlantic for the climate system and the sea level, most of the interior flow field is only known qualitatively, and neither the mean nor the variability and trends are quantified. In a long-term study, we investigated the current field in the western North Atlantic at 47°N between 44°W and 31°W using a combination of inverted echo sounders deployed at the seafloor and moored current meters (Rhein et al., 2019).

The North Atlantic Current (NAC) is only about 100–150 km wide but imports 106 Sv ($1 \text{ Sv} = 10^6 \text{ m}^3/\text{s}$) into the Newfoundland basin (Figure 81), making the NAC one of the strongest currents in the world ocean. Constrained by the bathymetry, more than half of the northward flow recirculates to the south in close proximity to the NAC (-59 Sv). The

mean transport of the southward boundary current at the continental margin is -23 Sv. The NAC and its return flow are significantly anti-correlated: A stronger NAC inflow corresponds to a stronger recirculation. The mean flow east of 37°W is -28 Sv to the south but much more sluggish than in the west and without permanent local features. This part of the circulation seems to be independent from the NAC system and the boundary current, since no significant correlation with these individual time series was found. The sum of the interior AMOC components results in a northward transport of 19 Sv. Combined with the southward boundary current the mean top-to-bottom transport across the measurement array is -4 Sv.

The temporal variability of the water transports across 47°N that was derived from the shipboard and the moored observations turned out to be highly correlated with sea surface height measurements from satellite altimetry, a result that was then used to calculate a longer time series of transport fluctuations directly from the altimeter measure-

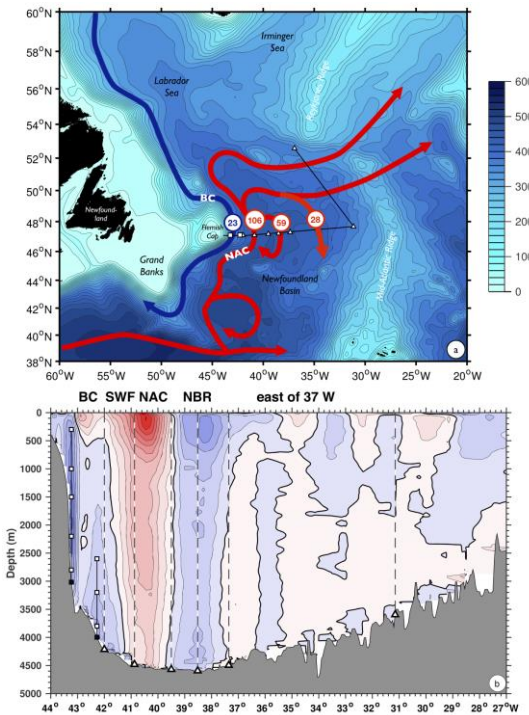


Figure 81: (a) Schematic circulation of the boundary current (blue) and the NAC system (red). Included are the locations of moored instruments and mean volume transports (in $10^6 \text{ m}^3/\text{s}$). (b) Mean meridional velocities at 47°N, based on 12 repeat lowered acoustic Doppler current profiler sections (red: northward, blue: southward velocities, contour lines are every 5 cm/s). The locations of the moorings (black squares) and pressure inverted echo sounders (triangles) are indicated, the current meters in the moorings are shown as white squares. The flow components are: BC = boundary current; SWF = southward flow; NAC = North Atlantic Current; NBR = Newfoundland Basin recirculation; east of 37°W = flow between 37°W and 31°W.

ments (Figure 82). The analysis reveals significant decadal trends (despite the large variability on all time scales), but these trends are found in the interior transport contribution and not in the Gulf Stream/NAC transport as might have been expected. The southward flow east of 37°W increased significantly by -0.44 Sv/year and is the main contributor to the declining interior northward flow of -0.60 Sv/year (Figure 82). Over the period of the analysis, the total transport in the interior decreased by about 10 Sv. The trends of the other individual components are not significant, but the sum of the interior and boundary current transport is -0.71 Sv/year.

The derived transport trends are linked to irregular decadal trends in sea surface height and thus most likely caused by regionally different warming of the water column. The decadal sea surface height trends (1993–2018) in the subpolar North Atlantic are generally positive and, at 47°N, strongest at the western boundary. In the interior, the trends are not significant at many locations, and patches of negative and positive trends are in close proximity along the perceived pathways of the NAC. Combined with the western boundary positive trend, this leads to a weakening horizontal pressure gradient and thus to decreasing interior northward transports from the subtropical to the subpolar western Atlantic.

References

McCarthy, G.D., P.J. Brown, C.N. Flagg, G. Goni, L. Houpert, C.W. Hughes, R. Hummels, M. Inall, K. Jochumsen, K.M.H. Larsen, P. Lherminier, C.S. Meinen, B.I. Moat, D. Rayner, M. Rhein, A. Roessler, C. Schmid, and D.A. Smeed, Sustainable observations of the AMOC: Methodology and Technology. *Reviews of Geophysics*, 58, e2019RG000654, doi:10.1029/2019RG000654, 2020.

Frajka-Williams, E., I.J. Anson, J. Baehr, H.L. Bryden, M. Paz Chidichimo, S.A. Cunningham, G. Danabasoglu, S. Dong, K.A. Donohue, S. Elipot, N.P. Holliday, R. Hummels, L.C. Jackson, J.

Karstensen, M. Lankhorst, I. Le Bras, S. Lozier, E.L. McDonough, C.S. Meinen, H. Mercier, B.I. Moat, R.C. Perez, C.G. Piecuch, M. Rhein, M. Skrokoz, K.E. Trenberth, S. Bacon, G. Forget, G. Goni, P. Heimbach, D. Kieke, J. Koelling, T. Lamont, G. McCarthy, C. Mertens, U. Send, D.A. Smeed, M. van den Berg, D. Volkov, and C. Wilson. Atlantic Meridional Overturning Circulation: Observed transports and variability. *Frontiers in Marine Science*, 6:260, doi:10.3389/fmars.2019.00260, 2019.

Rhein, M., Taking a close look at ocean circulation. *Science*, 363, 456-457, doi:10.1126/science.aaw3111, 2019.

Rhein, M., Mertens, C., and A. Roessler, Observed transport decline at 47°N, western Atlantic. *Journal of Geophysical Research: Oceans*, 124, doi:10.1029/2019JC014993, 2019.

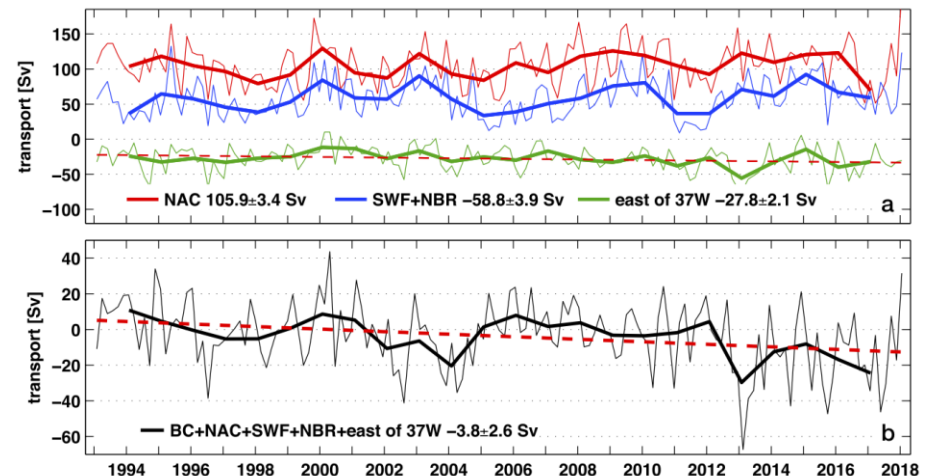


Figure 82: Time series of bimonthly (thin) and annual (bold) top-to-bottom mean transport (Sv) at 47°N. Long-term linear trends are indicated where statistically significant (dashed). (a) NAC (red), return flow (blue), and transport east of 37°W (green). The return flow is inverted to emphasize the high anti-correlation. (b) Sum of all transport contributions. Numbers are the mean transports and the standard error of the mean. NAC = North Atlantic Current; SWF = Southward Flow; NBR = Newfoundland Basin recirculation; BC = boundary current.